Application of cadherin cRNA probes in brains of Alzheimer's disease mouse model

He Zhou[a, b], Shijia Du[a], Fred Gendi[c], Haoyue Li[a], Jia Fu[a], and Cheng Chang[a, d, *]

[a] *School of Basic Medicine, Zhengzhou University, Zhengzhou, China*

[b] *Department of General and Visceral Surgery, Goethe University Hospital, Frankfurt am Main, Germany*

[c] *Uganda Christian University, P.O.Box 4, Mukono, Uganda*

[d] *Center of Cerebral Palsy Surgical Research and Treatment, Zhengzhou University, Zhengzhou, China*

**e-mail: changcheng@zzu.edu.cn*

The cadherin superfamily molecules, functioning as cell adhesion molecules, are recognized to play roles in both physiological and pathological processes. The cadherin-based adherent junction (CAJ) is believed to interact with presenilin-1 (PS-1), suggesting that disruptions in CAJ structures might contribute to neurodegeneration, potentially leading to Alzheimer's Disease (AD). Yet, the specific expression patterns of cadherin superfamily mRNA remain somewhat ambiguous. This research utilizes *in situ* Hybridization (ISH) to examine the expression and localization of cadherin mRNA in AD mouse model brains. Long cRNA probes targeting cadherin revealed endogenous mRNA expression in brain sections. Interestingly, senile plaques in the AD mouse brain are also bound to these probes. This binding, however, may not exclusively denote cadherin mRNA, as ISH detected both antisense and sense cRNA probes. Our data suggests that while antisense cRNA probes effectively detect cadherin mRNA expression in AD brain cells, their association with senile plaques might not specifically signify cadherin mRNA expression.

Keywords: Alzheimer's disease, cadherin, *in situ* hybridization, cRNA probe, senile plaques

INTRODUCTION

Alzheimer's disease (AD) is a kind of neurodegenerative disease characterized by the formation of senile plaques, neurofibrillary tangles (NFT), diffused brain atrophy, and reduction of neurons in the cerebral cortex and hippocampus. These pathological hallmarks are concomitant with progressive deficits in memory and cognitive functions [1, 2]. Mutations in amyloid precursor protein (APP) or presenilin (PS) genes have been linked to familial early-onset AD [3].

Cadherin superfamily molecules play pivotal roles in processes such as cell adhesion, cell signal interactions, synapse maturation, and cell polarity control. Disruptions in these processes

are observed in conditions like neuroinflammation and neurodegeneration [4, 5]. Changes of PS-1/ γ-secretase activity can lead to cell-cell adherent junctions' dissociation. Some studies indicate a physical interaction between PS-1 and E-cadherin, wherein PS-1 competes with p120 for E-cadherin binding. Moreover, there is a colocalization of PS1 and N-cadherin at the cell contacting junctions. Such observations suggest that cadherin-based adherent junction (CAJ) might physically interact with PS -1, potentially shedding light on the pathological onset of AD. The CAJ structural disorders might cause neurodegeneration that leads to Alzheimer's disease [6, 7]. Nonetheless, the specific role cadherin assumes within cortical lesions of AD needs further investigation.

In situ hybridization (ISH) serves as an invaluable tool to visualize gene expression at lesion sites. By employing specific oligonucleotide/DNA/RNA probes, ISH facilitates the direct localization of target gene mRNA expression within the brains of AD patients and transgenic models. This technique can pinpoint the regional distribution of cells expressing special mRNAs and provide morphological information about mRNA expression [8-10]. The cellular expressing localization patterns of AD-related genes were ß-amyloid, tau, presenilin-1, and ß-site APP cleaving enzyme on mRNA level were investigated by ISH and these studies provided mRNA distribution data for further analysis [11-15]. Various mRNA signals can display distinct distributions across the neuropil, neuronal bodies, and dendrites [11]. Therefore, ISH provides important distribution information on target mRNAs. Some previous studies have indicated that ISH probes may bind to senile plaques in AD patient brains, leading to the hypothesis that these plaques contain mRNAs [16, 17]. However, despite its widespread use, the reliability of ISH results using cRNA probes in neuronal cells and extracellular senile plaques of AD brains remains an area of uncertainty.

This study aimed to evaluate the utilization of cadherin superfamily long cRNA probes in the pathological progression of AD neurodegeneration. We assessed the mRNA expression and localization of various cadherin superfamily members in AD model mouse brains (APP/PS1 transgenic mice). Data concerning cadherin and proto-cadherin molecules that exhibited relatively pronounced expression in mouse brains were collated for this article. Differently labeled probes for mice and probes designed for another species (chicken, Gallus gallus domesticus) were employed to determine the efficacy of ISH both intracellularly and extracellularly. Our findings revealed that the extracellular interaction of long cRNA probes with senile plaques did not produce a distinct ISH pattern. However, the AD model demonstrated endogenous cadherin expression patterns in the brain that aligned with those observed in wild-type mice, reinforcing that ISH was still a classical technique for intracellular mRNA research.

MATERIALS AND METHODS

Experimental animals and groups. APP/PS1 transgenic mice and age-matched wild-type mice were employed in this study. These mice were generously provided by Dr. Christoph Kaether Leibnitz Institute of Age Research- Fritz Lipmann Institute, Germany [18]. All mice were kept under standard animal care conditions and were fed ad libitum.

Both transgenic and age-matched wild-type mice, at 3, 6, 9, and 12 months old, were anesthetized and subsequently decapitated. Dissections were conducted on ice. Brains were swiftly removed, frozen in about -40°C 2-methylbutane, and stored at -80°C until cryostat sectioning. The research complied with national and institutional guidelines, ensuring the minimum number of animals were used and all efforts were made to reduce animal distress.

Brain tissues were sliced into 20 μm thickness coronal sections in a cryostat (Microm). One adjacent slide of each series was stained with thionin to delineate basic neuronal structures.

cRNA Probes Synthesis. Antisense and sense cRNA probes for cadherin and proto-cadherin molecules were synthesized in vitro using the plasmids listed in Table 1. The plasmid DNA was linearized with restriction enzyme and purified using sodium acetate and alcohol at -80°C for 2 hours. After centrifugation at 14,000 x g for 20 minutes at 4°C, the supernatant was discarded. The resulting pellet was washed with 500μl pre-cold 70% ethanol, followed by another centrifugation under the same conditions. The pellet was left to air-dry and then dissolved in 25μl TE. The concentration was then determined by an ultraviolet spectrophotometer and the DNA was checked by agarose gel electrophoresis. The probes were synthesized with the Digoxigenin (Dig) RNA Labeling Kit (Roche Diagnostics) and the Fluorescein (Fluo) RNA Labeling Kit (Roche Diagnostics).

Table 1. Parameters of probes for cadherins

Name	Plasmid	Position of sequence	The GenBank accession number
Cdh2	bMN3-KS+mNCdh	333–1313*	NM_007664.4
Cdh4	pBSMR4	55-2794	D14888
Cdh6	pBSII1.0B-mCdh6	202-1229	D82029
Cdh7	TOPOII-mCdh7	182-1998	AK137369
Cdh8	mcad8-12	504-1583	X95600
Pcdh1	pGEMte-mPcdh1	1195-2781	NM029357
Pcdh8	TOPOII-mPcdh8	201-1901	NM_001042726.1
Pcdh17	TOPOII-mPcdh17	4787-6491	NM_001013753.2
Pcdh17-1	TOPOII-mPcdh17-1	2692-3607	NM_001013753.2
Pcdh17-2	TOPOII-mPcdh17-2	4787-5671	NM_001013753.2

Pcdh17-3	TOPOII-mPcdh17-3	5619-6491	NM_001013753.2
Chicken ß-actin	TOPOII-cActb	28-846	NM_205518.1

* probe for Cdh2 is a kind gift of Dr. M. Takeichi (RIKEN Center for Developmental Biology, Kobe, Japan).

***In situ* Hybridization (ISH).** The ISH was performed according to the procedure described previously [19]. Cryostat sections were fixed in 4% paraformaldehyde, followed by rinsing with phosphate-buffered saline (PBS). Subsequently, the sections were treated with 1 μg/ml proteinase K (Sigma-Aldrich) and 0.25% acetic anhydride. Hybridization with cRNA probes (about 300ng/slide) was conducted overnight at 70°C. Then the sections were washed in 5× saline-sodium citrate buffer (SSC) followed by 2× SSC solution at 60°C. After RNase A (20 μg/ml, Sigma-Aldrich) treatment, slides were sequentially rinsed with 2×SSC and 0.1×SSC solution at room temperature. 2% heat-inactivated sheep serum was employed to reduce nonspecific binding. Alkaline phosphatase-coupled anti-digoxigenin Fab fragments (anti-Dig-Fab AP, Roche Diagnostics) were applied, with an overnight incubation at 4°C. Target mRNA visualization was achieved by incubating sections with a substrate solution consisting of 0.03% nitroblue tetrazolium (NBT) and 0.02% 5-bromo-4-chloro-3-indolyl-phosphate (BCIP) for 1 to 3 days at either 4°C or room temperature. Sections were methodically dehydrated using a gradient alcohol series, equilibrated by xylene, and mounted with Entellan (Merck Millipore).

Double *in situ* Hybridization (DISH). Some steps in the above ISH protocol were modified for DISH. Sections were first fixed in 4% paraformaldehyde for 2 hours, followed by treatment with proteinase K (1 μg/ml, Sigma-Aldrich) and 0.25% acetic anhydride. Slides were hybridized with a mixture of Dig- and Fluo-labeled cRNA probes overnight at 70°C. Subsequent washing steps included a rinse in 5×SSC and 50% formamide/1×SSC at 60 °C. Post RNase A treatment, slides were sequentially rinsed with 2×SSC and 0.2×SSC at 60 °C. Blocking was achieved using with 5% heat-inactivated sheep serum (Sigma-Aldrich) and 2% blocking reagent (Roche Diagnostics). The sections were then incubated with anti-Dig-Fab AP at room temperature for 2 hours to detect digoxigenin-labeled probes, followed by incubation with NBT/BCIP substrate solution. Detection of the fluorescein-labeled probes involved an overnight incubation with alkaline phosphatase-coupled anti-fluorescein Fab fragments (anti-Fluo-Fab AP, Roche Diagnostics) at 4°C. After washing, sections were treated with Fast Red chromogen (0.1 mg/ml, Roche).

Double-Fluorescence Labeling (FISH+FIHC). Fluorescence *in situ* Hybridization (FISH): The ISH protocol described previously was employed with one alteration. The chromogenic reagent was substituted with a solution containing Fast Red (0.1 mg/ml, Roche Diagnostics), which was allowed to develop at 4°C overnight.

Fluorescence Immunohistochemistry Staining (FIHC): Subsequent to the FISH procedure, sections were fixed in 4% paraformaldehyde for 20 minutes and then rinsed with Tris-buffered saline (TBS). For blocking, sections were treated with TBS supplemented with 5% goat serum. Slides were then incubated with mouse anti- Aß3552 (1:1000, rabbit-anti-mouse Aß1-40, a kind gift from Dr. Kaether's group) [20]. Detection was achieved using Alexa Fluor-488-conjugated secondary antibody (1:300, Millipore). As a final step, sections were counterstained with the nuclear dye Hoechst 33342 (1:30000, Sigma Aldrich) for 5 minutes.

Immunohistochemistry Staining (IHC). Sections were initially fixed in 4% paraformaldehyde. To inhibit endogenous peroxidase activity, they were treated with 0.3% H_2O_2 in methanol for 30 minutes. Following a blocking step using 5% goat serum, the sections were incubated with mouse anti- Aß 3552 (1:1000). This was followed by treatment with a biotin-conjugated secondary antibody (1:300, goat-anti-rabbit, Jackson ImmunoResearch). Detection was accomplished using TBS supplemented with 0.05% 3,3-diaminobenzidine, 0.04% nickel chloride, and 0.01% H_2O_2.

Image Analysis. All sections were visualized using a transmission light microscope (BX40, Olympus). Image capture was performed with an Olympus DP70 digital camera and a confocal laser scanning microscope (SP5, Leica Microsystems). Necessary adjustments of contrast and brightness in images were achieved through Photoshop software (Adobe).

RESULTS

ISH revealed that cadherin transcripts were widely distributed in APP/PS1 transgenic mouse brain. The regions of cadherin mRNA expression largely aligned with those observed in the wild-type mouse brain. Distinct expression levels of various cadherin molecules were noted in specific regions and subregions, including the cerebral cortex, basal ganglia, hippocampus, thalamus, and hypothalamus (Fig. 1 and Fig. 2). Concurrently, an interaction between cRNA probes and senile plaques was observed in the AD model mouse brains.

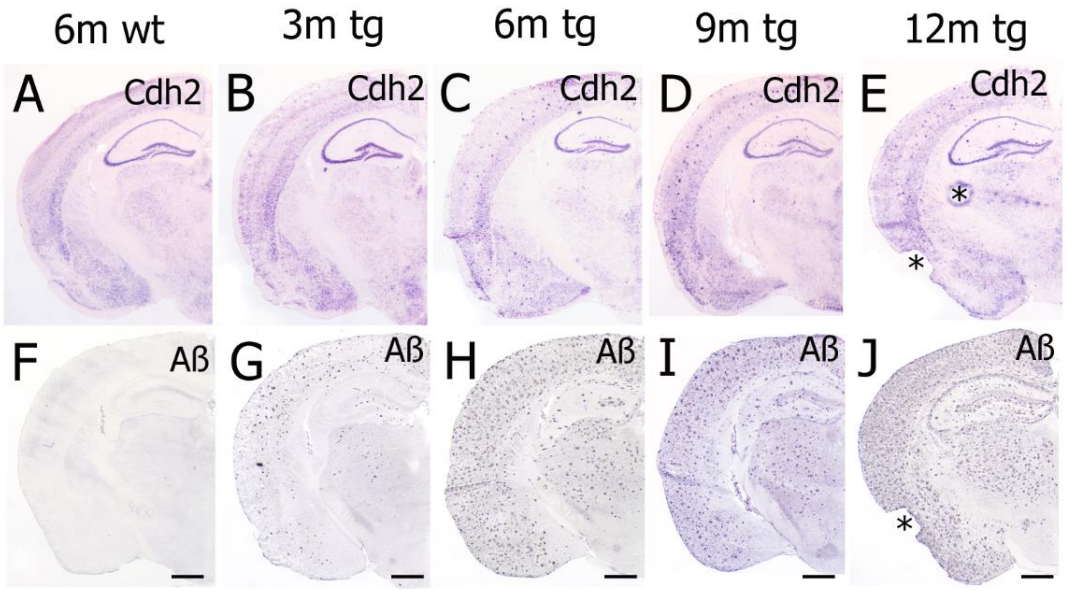

Fig. 1. ISH results of Cdh2 cRNA probes and the expression of ß-amyloid peptide 1-40 detected by IHC in transgenic and wild-type mouse brain in respective stages. (A, F) 6-month-old wild-type mouse. (B, G) 3-month-old transgenic mouse. (C, H) 6-month-old transgenic mouse. (D, I) 9-month-old transgenic mouse. (E, J) 12 months old transgenic mouse. TG, transgenic mouse. WT, wild-type mouse. The asterisks indicate artifacts. Scale bar = 1 mm.

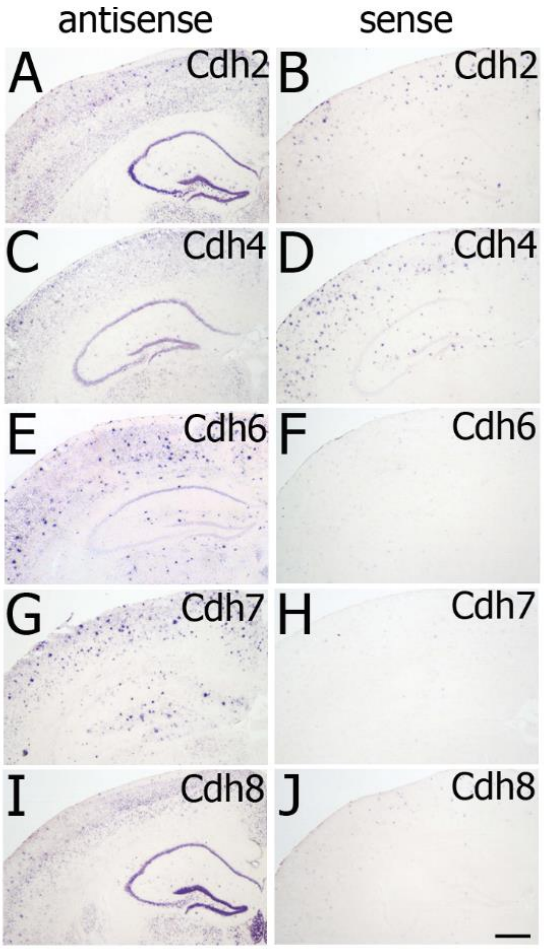

Fig. 2. ISH signal for antisense and sense cRNA probes of cadherins in AD model. (A, B) Cdh2 antisense and sense cRNA probes. (C, D) Cdh4 antisense and sense cRNA probes. (E, F) Cdh6 antisense and sense cRNA

probes. (G, H) Cdh7 antisense and sense cRNA probes. (I, J) Cdh8 antisense and sense cRNA probes. Plaques were detected by some probes in A, B, D, E, and G. Antisense, antisense probes. Sense, sense probes. Scale bar = 500 μm.

Endogenous expression of Cadherins.

The Cdh2 mRNA regional expression in 3, 6, 9, and 12-month-old transgenic mice brains was comparable to that of 6-month-old wild-type mice (Fig. 1). Sections of 6-month-old mice are presented in Fig.2-6. Thioning staining was utilized to delineate the anatomical structures in both the AD model and wild-type mice (Fig. 3 A, -C). Overall, both transgenic and wild-type adult mice showcased analogous endogenous cadherin mRNA expression patterns and consistent

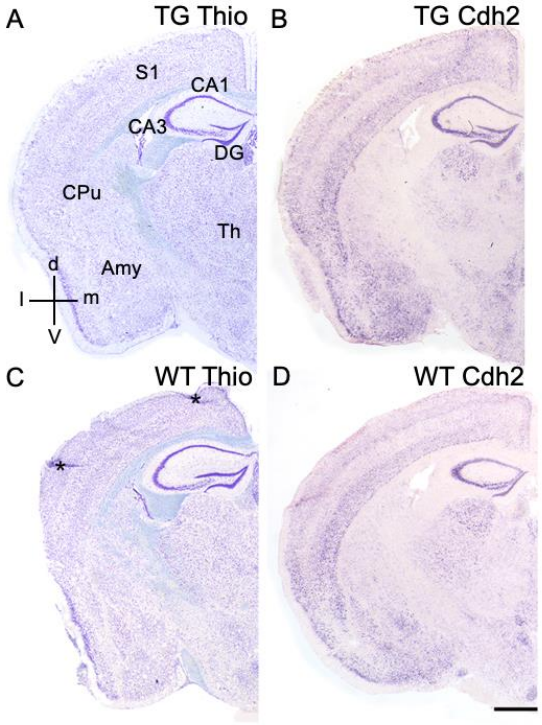

Thioning staining in their brains (Fig. 1 and Fig. 3)

Fig. 3. The thionin staining and Cdh2 mRNA expression in adult AD mouse model and wild-type mouse brains. (A, C) Results of thionin staining. (B, D) The ISH results of Cdh2 cRNA probes. Abbreviations are CA1, field CA1 of hippocampus; CA3, field CA3 of hippocampus; DG, dentate gyrus; S1, primary somatosensory cortex; CPu, Caudate Putamen; Amy, amygdala; Th, thalamus. d, dorsal; v, ventral; l, lateral; m, medial. TG, transgenic mouse; WT, wild-type mouse. The asterisks indicate artifacts. Scale bar = 1 mm.

Plaque staining by ISH, IHC, and Double-Fluorescence Labeling.

ISH results indicated significant deposition accumulation in the transgenic mouse brain, detectable by both cRNA antisense probes and sense probes (Fig. 2). In contrast, the wild-type

mouse brain showed no evident plaque staining (Fig. 1A). This deposition was primarily found in the cortex, hippocampus, and thalamus, though staining patterns varied based on the probes used (Fig. 1B-E and Fig. 2).

Given the possibility that the deposition could represent senile plaques, an antibody against Aß1-40 was utilized to assess the properties of these plaques (Fig. 1F-J). The IHC staining outcomes using the Aß1-40 antibody paralleled those of ISH results obtained with cRNA probes (Fig. 1). Analogous results were noted in the somatosensory cortex using antisense probes for Cdh6, Cdh8, Pcdh8, and Aß antibody (Fig. 4). While plaques stained by the Pcdh8 antisense probe aligned with the location of Aß plaques as revealed by a double-labeling technique, not all plaques bound probes (Fig. 4A-C).

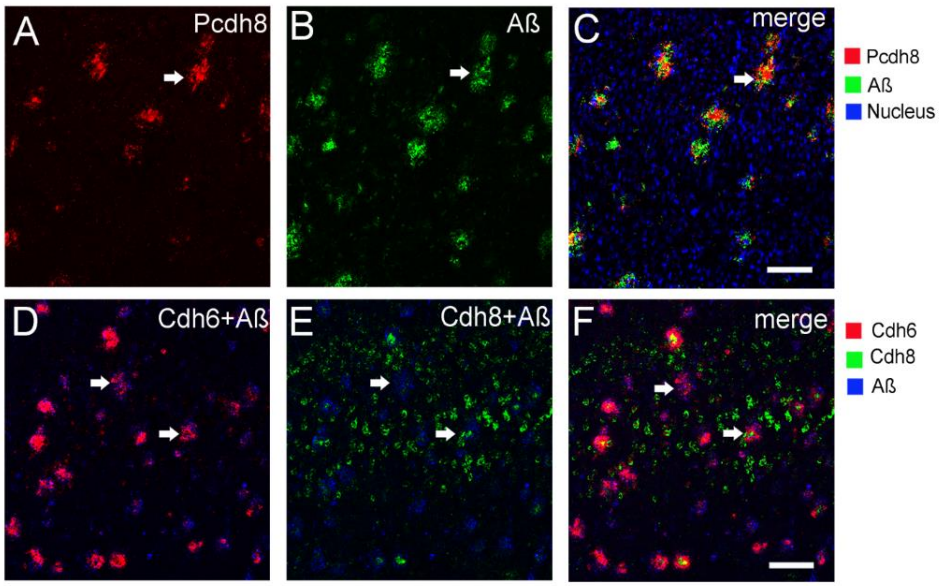

Fig. 4. The double-fluorescence labeling for Pcdh8 antisense probe and Aß antibody (A-C) and the DISH plus FIHC results for Cdh6 antisense probe, Cdh8 antisense probe and Aß antibody (D-F) in somatosensory cortex. These results are from adult transgenic mouse brain sections. The arrows indicate a double-stained plaque in A-C and the blue fluorescence represents nuclear staining (Hoechst 33342) in C. The senile plaques were green color counterstained in B and C and blue color in E and F by using aßAß1-40 antibody. The upper arrow indicates a double stained plaque in D-F and the lower arrow indicates a triple stained plaque in D-F. Scale bars = 200 µm.

Double fluorescence in situ hybridization.

In layer II and III of somatosensory cortex, the antisense probe for Cdh8 only bound a few plaques. In contrast, the antisense probe for Cdh6 showed binding to a significantly greater number of plaques compared to that of Cdh8 (Fig. 4D-4F). These observations suggest that the

binding patterns between cRNA probes and senile plaques may vary based on the specificity of the probe used.

In situ hybridization for fragmental cadherin mRNAs.

To determine if cadherin mRNAs were specifically entrapped in plaques, we constructed three primer pairs targeting distinct regions of the mouse Pcdh17 cDNA coding sequences. Subsequent probes corresponding to these Pcdh17 cDNA fragments were then synthesized. ISH findings revealed that while these new probes exhibited endogenous expression patterns akin to the full-length probe, their plaque staining patterns differed (Fig. 5). Such outcomes suggest that the probes might not specifically bind to target mRNA within the senile plaques, indicating that the interaction between cRNA probes and senile plaques was non-specific.

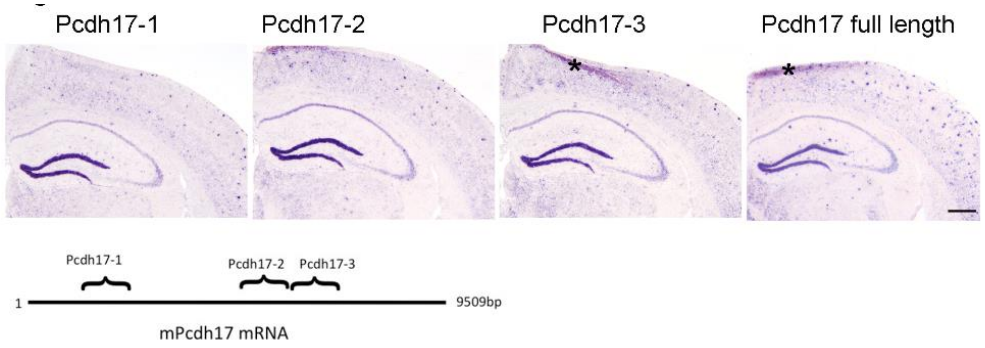

Fig. 5. The ISH results of the new probes for different parts of Pcdh17 coding sequences. (A) New probe for Pcdh17 fragment Pcdh-1. (B) New probe for Pcdh17 fragment Pcdh-2. (C) New probe for Pcdh17 fragment Pcdh-3. (D) New probe for full-length Pcdh17 (a combination of fragments Pcdh-2 and 3). The schematics show the locations of the three fragmental probes of Pcdh17 mRNA. The asterisks show artifacts in C and D. Scale bar = 500 μm. d.

Results of control ISH experiments.

The sense probes' absence of a positive signal in wild-type mouse brain sections confirmed the specificity of our antisense probes in targeting various cadherin mRNAs within the cytoplasm (Fig. 6A-B). Notably, both antisense and sense probes were found to bind to senile plaques in the brains of transgenic mice (Fig. 3). Fluorescent-labeled probes displayed similar staining for plaques to those of digoxigenin-labeled probes, suggesting that the interaction occurs between cRNA and senile plaques (Fig. 6C). The cRNA probe designed for chicken ß-actin also displayed plaque staining (Fig. 6D). ISH analyses on RNase-treated sections revealed that plaques still bound to cRNA probes, even when RNA was digested within the tissue (Fig. 6E-F). In other control experiments, the probe-blank ISH and the dual blank of both probe and antibody experiment resulted in very faint plaque staining (Fig. 6G-H). This underscores that the distinct

intensity of plaque staining patterns is influenced by the specific characteristics of the respective probes.

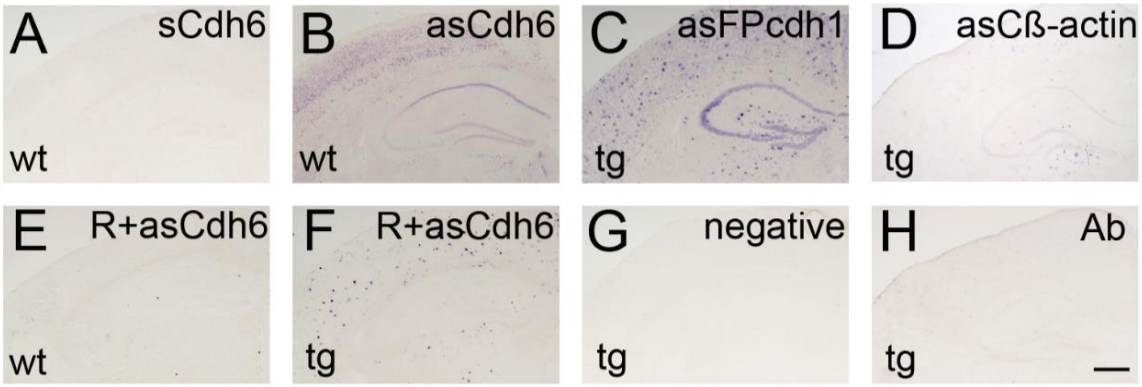

Figure 6. Results of specificity tests. (A, B) ISH specificity tests by mouse Cdh6 probes. Cdh6 mRNA hybridization signal in sections of wild-type mouse brain by using sense (A) or antisense (B) digoxigenin-labeled cRNA probe. ISH test by antisense fluorescent-labeled probe of mouse Pcdh1 (C) and antisense digoxigenin-labeled probe of chicken ß-actin (D). (E, F) ISH test after Rnase A pretreatment by antisense Cdh6 probe. Sections are from wild-type mouse (E) and transgenic mouse (F). (G, H) ISH control experiments in sections of transgenic mouse brain. A negative control including no probe or antibody (G). Another negative control includes no probe but antibody (H). sCdh6, sense probe of Cdh6; asCdh6, antisense probe of Cdh6; asFPcdh1, antisense fluorescent-labeled probe of Pcdh1; asCß-actin, antisense digoxigenin-labeled probe of chicken ß-actin; R, Rnase A pretreatment; Ab, anti-digoxigenin antibody. Scale bar = 500 μm.

DISCUSSION

This study aimed to validate the application of long cRNA probes in investigating the brains of Alzheimer's disease mouse models and to further elucidate the role of cadherin mRNA in the pathogenesis of Alzheimer's disease.

As anticipated, ISH localized the intracellular expression of cadherin mRNAs in AD models. The experimental procedure was meticulously and thoroughly conducted. Staining was consistently done at 4°C. To minimize variability, all slides from both wild-type and transgenic mice, used for antisense and sense probes of a given molecule, underwent the same staining duration. The congruent endogenous cadherin expression patterns and thioning staining results between adult AD model mouse brains and wild-type mouse brains suggest that not all neurons were severely compromised by the progressive neurodegenerative changes associated with AD. Furthermore, these findings affirm that ISH remains a robust and refined technique for pinpointing intracellular mRNA expression and localization.

Our initial ISH results revealed a significant deposition in the brains of transgenic mice, detectable by long cadherin cRNA probes. The Aß1-40 antibody was used for IHC, and it was

determined that the plaques stained by ISH coincided with Aß peptide locations as verified by a double-labeling technique. However, not all plaques could bind cRNA probes. Some researchers propose that probes bind to target mRNAs and the extent of probe binding may be influenced by the maturity of the plaques. Denser, more mature senile plaques possess a lower mRNA concentration compared to those primitive plaques and diffuse plaques, indicating that mature plaques might have a reduced mRNA binding capacity relative to their less mature counterparts [21]. Earlier research indicated that various types of Aß peptides might accumulate intracellularly, disrupting physiological processes and eventually leading to cell death. Consequently, all cellular structures would be released into the extracellular space [22]. Nucleic acids have been found to aid in the formation of amyloid from short peptides [23]. In previous study, this was perceived as a specific interaction where RNAs could become entrapped in both neurofibrillary tangles and senile plaques. Moreover, numerous mRNAs had been detected within individual senile plaques from AD brains using techniques such as ISH, acridine orange histochemistry, and reverse northern blotting. However, one group employed an excess of unlabeled antisense probes as controls for ISH. Thus, it was difficult to confirm the specificity of ISH-detected bindings to target mRNAs [24-26].

Other researchers have argued that it's not mRNAs, but rather unidentified components, that bind with the cRNA probes, yet this challenges the earlier viewpoint that target mRNAs were sequestered in senile plaques [15]. In our experiments, senile plaques could bind both antisense and sense probes for various mouse cadherins. They were also able to bind Fluorescent-labeled probes, antisense probes for chicken ß-actin, and digoxigenin-labeled mouse cadherin probes, suggesting the possibility of unspecific binding. Even RNase pretreated sections exhibited plaque staining following the ISH procedure. This reinforces the idea that not all binding components in the senile plaque are mRNA, and the binding might not be RNA-specific. Nonetheless, this concept requires further chemical analysis. The varying results from different antisense probes in DISH suggest that the binding may be influenced by the unique compositions of each probe.

Some probes exhibited reduced binding results compared to others, possibly because they were only able to recognize matured plaques or plaques in the late stage. Consequently, these probes displayed diverse ISH staining outcomes for plaques [21]. Notably, the ISH outcomes for new probes designed for fragments of mouse Pcdh17, which displayed endogenous expression patterns resembling full-length probes, did not mirror the plaque staining patterns. This suggests that plaque staining is not contingent on endogenous expression and further hints at a potential non-specific interaction between senile plaques and cadherin cRNA probes. These findings underscore that interactions between probes and senile plaques are influenced by distinctive

probe characteristics, primarily their composition. The unidentified constituents in plaques that interacted with cRNA probes may be RNA-binding proteins (RBPs). These proteins play pivotal roles in the post-transcriptional regulation of mRNAs and are believed to participate in the translation of APP [27]. For instance, a 3kb APP transcript can interact with several RNA-binding proteins, such as the fragile X mental retardation protein and iron regulatory proteins, at its 3' untranslated regions (3'-UTR), 5'-UTR, and coding region. These RNA-binding proteins could potentially contribute to the formation of senile plaques [28]. In our research, the probes we employed were considerably longer (around 1000bp) than those used by other teams (20-100bp) [9, 15, 24]. Long probes in terms of ISH can offer enhanced sensitivity compared to shorter ones. Additionally, RNA probes tend to have a stronger hybridization affinity to target mRNA molecules than DNA probes [29, 30]. Conversely, these longer cRNA probes may present more available binding sites for RNA-binding proteins compared to their shorter counterparts [31]. Scientists have postulated that Aß might establish direct interactions with RNA through its ß-hairpin structure [32].

While ISH results demonstrated non-specific extracellular binding between cRNA probes and senile plaques, given that both sense and antisense probes of various cadherins could bind, our findings of comparable endogenous cadherin expression patterns between transgenic mice and wild-type mice underscore ISH is still a classical technique for studying intracellular mRNA expression and localization. Still, we cannot dismiss potential links between cadherin and AD-associated proteins such as APP, presenilin, and apolipoprotein E [33-35]. The roles of individual cadherin mRNAs in AD-associated neurodegeneration merit separate analyses. Beyond merely detecting cellular expression and localization, ISH might not stand alone as the definitive method to investigate the interplay between cadherin mRNAs and AD senile plaques or extracellular Aß. Tools like quantitative real-time PCR, microarray analysis, and single cell sequencing provide alternative means to quantify gene expression in AD research, which can offer insights into gene expression from diverse brain regions [36-41]. Continued exploration in this arena remains essential for future discoveries.

ACKNOWLEDGMENTS

This work was supported by the Anatomy I Institute of the University of Jena. The author thanks Dr. Kaether, Prof. Dr. Jucker, and Prof. Dr. Haass and their groups for the mouse model and antibodies and Dr. F. van Roy, Dr. M. Takeichi, Dr. T. Jessell and Dr. H. Cremer for some plasmids. All authors participated in this study and have access to all data in this work.

FUNDING

This study is supported by the Scientific and Technological Research Project of Henan Provincial Department of Science and Technology (Grant No. 212102310217) and the grant from Funds of the National Natural Science Foundation of China (Grant No. 81401015).

CONFLICT OF INTEREST

The authors declare that they have no conflicts of interest.

AUTHOR CONTRIBUTION

H.Z. conceived of the study and designed the study; H.Z. and S.D. collected, analyzed the data, and wrote the initial draft of the paper; C.C. carried the project administration and supervision; all authors contributed to carrying out additional analyses and revising the manuscript.

REFERENCES

1. Iqbal K, Grundke-Iqbal I, Zaidi T, Merz PA, Wen GY, Shaikh SS, Wisniewski HM, Alafuzoff I, Winblad B (1986). Defective brain microtubule assembly in Alzheimer's disease. *Lancet*; **2**(8504): 421-6.

2. Sherrington R, Rogaev EI, Liang Y, Rogaeva EA, Levesque G, Ikeda M, Chi H, Lin C, Li G, Holman K, Tsuda T, Mar L, Foncin JF, Bruni AC, Montesi MP, Sorbi S, Rainero I, Pinessi L, Nee L, Chumakov I, Pollen D, Brookes A, Sanseau P, Polinsky RJ, Wasco W, Da Silva HA, Haines JL, Perkicak-Vance MA, Tanzi RE, Roses AD, Fraser PE, Rommens JM, St George-Hyslop PH (1995). Cloning of a gene bearing missense mutations in early-onset familial Alzheimer's disease. *Nature*; **375**(6534): 754-60.

3. Bagyinszky E, Youn YC, An SSA, Kim S (2016). Mutations, associated with early-onset Alzheimer's disease, discovered in Asian countries. *Clinical Interventions in Aging*; **11**: 1467-88.

4. Unger MS, Schernthaner P, Marschallinger J, Mrowetz H, Aigner L (2018). Microglia prevent peripheral immune cell invasion and promote an anti-inflammatory environment in the brain of APP-PS1 transgenic mice. *Journal of Neuroinflammation*; **15**.

5. Weiner MW, Veitch DP, Aisen PS, Beckett LA, Cairns NJ, Cedarbaum J, Green RC, Harvey D, Jack CR, Jagust W, Luthman J, Morris JC, Petersen RC, Saykin AJ, Shaw L, Shen L, Schwarz A, Toga AW, Trojanowski JQ, Alzheimer's Disease Neuroimaging I (2015). 2014 Update of the Alzheimer's Disease Neuroimaging Initiative: A review of papers published since its inception. *Alzheimer's & dementia : the journal of the Alzheimer's Association*; **11**(6): e1-120.

6. Widelitz R (2005). Wnt signaling through canonical and non-canonical pathways: Recent progress. *Growth Factors*; **23**(2): 111-6.

7. Giagtzoglou N, Ly CV, Bellen HJ (2009). Cell Adhesion, the Backbone of the Synapse: "Vertebrate" and "Invertebrate" Perspectives. *Cold Spring Harbor Perspectives in Biology*; **1**(4).

8. Wegenast-Braun BM, Maisch AF, Eicke D, Radde R, Herzig MC, Staufenbiel M, Jucker M, Calhoun ME (2009). Independent Effects of Intra- and Extracellular A beta on Learning-Related Gene Expression. *American Journal of Pathology*; **175**(1): 271-82.

9. Melchior B, Garcia AE, Hsiung BK, Lo KM, Doose JM, Thrash JC, Stalder AK, Staufenbiel M, Neumann H, Carson MJ (2010). Dual induction of TREM2 and tolerance-related transcript, Tmem176b, in amyloid transgenic mice: implications for vaccine-based therapies for Alzheimer's disease. *Asn Neuro*; **2**(3): 157-70.

10. Lehmann SM, Kruger C, Park B, Derkow K, Rosenberger K, Baumgart J, Trimbuch T, Eom G, Hinz M, Kaul D, Habbel P, Kalin R, Franzoni E, Rybak A, Nguyen D, Veh R, Ninnemann O, Peters O, Nitsch R, Heppner FL, Golenbock D, Schott E, Ploegh HL, Wulczyn FG, Lehnardt S (2012). An unconventional role for miRNA: let-7 activates Toll-like receptor 7 and causes neurodegeneration. *Nature Neuroscience*; **15**(6): 827-U44.

11. Neve RL, Valletta JS, Li Y, Ventosa-Michelman M, Holtzman DM, Mobley WC (1996). A comprehensive study of the spatiotemporal pattern of beta-amyloid precursor protein mRNA and protein in the rat brain: lack of modulation by exogenously applied nerve growth factor. *Brain Res Mol Brain Res*; **39**(1-2): 185-97.

12. Aronov S, Aranda G, Behar L, Ginzburg I (2001). Axonal tau mRNA localization coincides with tau protein in living neuronal cells and depends on axonal targeting signal. *Journal of Neuroscience*; **21**(17): 6577-87.

13. Malmqvist T, Anthony K, Gallo JM (2014). Tau mRNA is present in axonal RNA granules and is associated with elongation factor 1A. *Brain Research*; **1584**: 22-7.

14. Page K, Hollister R, Tanzi RE, Hyman BT (1996). In situ hybridization analysis of presenilin 1 mRNA in Alzheimer disease and in lesioned rat brain. *Proceedings of the National Academy of Sciences of the United States of America*; **93**(24): 14020-4.

15. Irizarry MC, Locascio JJ, Hyman BT (2001). beta-site APP cleaving enzyme mRNA expression in APP transgenic mice - Anatomical overlap with transgene expression and static levels with aging. *American Journal of Pathology*; **158**(1): 173-7.

16. Pardue S, White CL, 3rd, Bigio EH, Morrison-Bogorad M (1994). Anomalous binding of radiolabeled oligonucleotide probes to plaques and tangles in Alzheimer disease hippocampus. *Mol Chem Neuropathol*; **22**(1): 1-24.

17. Ginsberg SD, Crino PB, Lee VM, Eberwine JH, Trojanowski JQ (1997). Sequestration of RNA in Alzheimer's disease neurofibrillary tangles and senile plaques. *Ann Neurol*; **41**(2): 200-9.

18. Radde R, Bolmont T, Kaeser SA, Coomaraswamy J, Lindau D, Stoltze L, Calhoun ME, Jäggi F, Wolburg H, Gengler S, Haass C, Ghetti B, Czech C, Hölscher C, Mathews PM, Jucker M (2006). Abeta42-driven cerebral amyloidosis in transgenic mice reveals early and robust pathology. *EMBO Rep*; **7**(9): 940-6.

19. Redies C, Engelhart K, Takeichi M (1993). Differential expression of N- and R-cadherin in functional neuronal systems and other structures of the developing chicken brain. *J Comp Neurol*; **333**(3): 398-416.

20. Yamasaki A, Eimer S, Okochi M, Smialowska A, Kaether C, Baumeister R, Haass C, Steiner H (2006). The GxGD motif of presenilin contributes to catalytic function and substrate identification of gamma-secretase. *J Neurosci*; **26**(14): 3821-8.

21. Marcinkiewicz M (2002). beta APP and furin mRNA concentrates in immature senile plaques in the brain of Alzheimer patients. *Journal of Neuropathology and Experimental Neurology*; **61**(9): 815-29.

22. Gouras GK, Almeida CG, Takahashi RH (2005). Intraneuronal A beta accumulation and origin of plaques in Alzheimer's disease. *Neurobiology of Aging*; **26**(9): 1235-44.

23. Friedrich RP, Tepper K, Roznicke R, Soom M, Westermann M, Reymann K, Kaether C, Fandrich M (2010). Mechanism of amyloid plaque formation suggests an intracellular basis of A beta pathogenicity. *Proceedings of the National Academy of Sciences of the United States of America*; **107**(5): 1942-7.

24. Ginsberg SD, Crino PB, Hemby SE, Weingarten JA, Lee VMY, Eberwine JH, Trojanowski JQ (1999). Predominance of neuronal mRNAs in individual Alzheimer's disease senile plaques. *Annals of Neurology*; **45**(2): 174-81.

25. Ginsberg SD, Alldred MJ, Che SL (2012). Gene expression levels assessed by CA1 pyramidal neuron and regional hippocampal dissections in Alzheimer's disease. *Neurobiology of Disease*; **45**(1): 99-107.

26. Uehara Y, Yamada T, Baba Y, Miura SI, Abe S, Kitajima K, Higuchi MA, Iwamoto T, Saku K (2008). ATP-binding cassette transporter G4 is highly expressed in microglia in Alzheimer's brain. *Brain Research*; **1217**: 239-46.

27. Westmark CJ, Malter JS (2007). FMRP mediates mGluR(5)-dependent translation of amyloid precursor protein. *Plos Biology*; **5**(3): 629-39.

28. Rogers JT, Bush AI, Cho HH, Smith DH, Thomson AM, Friedlich AL, Lahiri DK, Leedman PJ, Huang XD, Cahill CM (2008). Iron and the translation of the amyloid precursor protein (APP) and ferritin mRNAs: riboregulation against neural oxidative damage in Alzheimer's disease. *Biochemical Society Transactions*; **36**: 1282-7.

29. Dona F, Houseley J (2014). Unexpected DNA Loss Mediated by the DNA Binding Activity of Ribonuclease A. *Plos One*; **9**(12).

30. Chartrand P, Bertrand E, Singer RH, Long RM. Sensitive and high-resolution detection of RNA in situ. In: Celander DW, Abelson JN, editors. Rna-Ligand Interactions, Part B: Molecular Biology Methods. Methods in Enzymology. 3182000. p. 493-506.

31. King OD, Gitler AD, Shorter J (2012). The tip of the iceberg: RNA-binding proteins with prion-like domains in neurodegenerative disease. *Brain Research*; **1462**: 61-80.

32. Mathura VS, Paris D, Ait-Ghezala G, Quadros A, Patel NS, Kolippakkam DN, Volmar CH, Mullan MJ (2005). Model of Alzheimer's disease amyloid-beta peptide based on a RNA binding protein. *Biochemical and Biophysical Research Communications*; **332**(2): 585-92.

33. Chen JW, Newhall J, Xie ZR, Leckband D, Wu YH (2016). A Computational Model for Kinetic Studies of Cadherin Binding and Clustering. *Biophysical Journal*; **111**(7): 1507-18.

34. Mills F, Globa AK, Liu S, Cowan CM, Mobasser M, Phillips AG, Borgland SL, Bamji SX (2017). Cadherins mediate cocaine-induced synaptic plasticity and behavioral conditioning. *Nature Neuroscience*; **20**(4): 540-+.

35. McCrea PD, Maher MT, Gottardi CJ. Nuclear Signaling from Cadherin Adhesion Complexes. In: Yap AS, editor. Cellular Adhesion in Development and Disease. Current Topics in Developmental Biology. 1122015. p. 129-96.

36. Gutala RV, Reddy PH (2004). The use of real-time PCR analysis in a gene expression study of Alzheimer's disease post-mortem brains. *J Neurosci Methods*; **132**(1): 101-7.

37. Veremeyko T, Starossom SC, Weiner HL, Ponomarev ED (2012). Detection of microRNAs in microglia by real-time PCR in normal CNS and during neuroinflammation. *J Vis Exp*; (65).

38. Acquaah-Mensah GK, Taylor RC (2016). Brain in situ hybridization maps as a source for reverse-engineering transcriptional regulatory networks: Alzheimer's disease insights. *Gene*; **586**(1): 77-86.

39. Kirouac L, Rajic AJ, Cribbs DH, Padmanabhan J (2017). Activation of Ras-ERK Signaling and GSK-3 by Amyloid Precursor Protein and Amyloid Beta Facilitates Neurodegeneration in Alzheimer's Disease. *Eneuro*; **4**(2).

40. Benedet AL, Milà-Alomà M, Vrillon A, Ashton NJ, Pascoal TA, Lussier F, Karikari TK, Hourregue C, Cognat E, Dumurgier J, Stevenson J, Rahmouni N, Pallen V, Poltronetti NM, Salvadó G, Shekari M, Operto G, Gispert JD, Minguillon C, Fauria K, Kollmorgen G, Suridjan I, Zimmer ER, Zetterberg H, Molinuevo JL, Paquet C, Rosa-Neto P, Blennow K, Suárez-Calvet M (2021). Differences Between Plasma and Cerebrospinal Fluid Glial Fibrillary Acidic Protein Levels Across the Alzheimer Disease Continuum. *JAMA Neurol*; **78**(12): 1471-83.

41. Ali M, Huarte OU, Heurtaux T, Garcia P, Rodriguez BP, Grzyb K, Halder R, Skupin A, Buttini M, Glaab E (2022). Single-Cell Transcriptional Profiling and Gene Regulatory Network Modeling in Tg2576 Mice Reveal Gender-Dependent Molecular Features Preceding Alzheimer-Like Pathologies. *Mol Neurobiol*.